



HAL
open science

Contact resistance optimization for development of thermoelectric modules based on bismuth telluride nanowires

Meriam Ben Khedim, Laurent Cagnon, Emmanuel André, Sébastien Pairis, Valerie Serradeil, Daniel Bourgault

► To cite this version:

Meriam Ben Khedim, Laurent Cagnon, Emmanuel André, Sébastien Pairis, Valerie Serradeil, et al.. Contact resistance optimization for development of thermoelectric modules based on bismuth telluride nanowires. AIP Advances, 2021, 11 (5), pp.055109. 10.1063/5.0043940 . hal-03331699

HAL Id: hal-03331699

<https://hal.science/hal-03331699>

Submitted on 2 Sep 2021

HAL is a multi-disciplinary open access archive for the deposit and dissemination of scientific research documents, whether they are published or not. The documents may come from teaching and research institutions in France or abroad, or from public or private research centers.

L'archive ouverte pluridisciplinaire **HAL**, est destinée au dépôt et à la diffusion de documents scientifiques de niveau recherche, publiés ou non, émanant des établissements d'enseignement et de recherche français ou étrangers, des laboratoires publics ou privés.

Contact resistance optimization for development of thermoelectric modules based on bismuth-telluride nanowires

Meriam Ben Khedim^{1,2,3}, Laurent Cagnon^{1,2}, Emmanuel André^{1,2}, Sébastien Pairis^{1,2}, Valerie Serradeil³ and Daniel Bourgault ^{*1,2}

(1) Univ. Grenoble Alpes, Institut Néel, F-38042 Grenoble, France.

(2) Centre National de la Recherche Scientifique / Institut Néel, 25 Avenue des Martyrs, BP 166, 38042 Grenoble Cedex 9, France

(3) Technology R&D, STMicroelectronics, 13106 Rousset, France

** Corresponding author ; E-mail : daniel.bourgault@neel.cnrs.fr*

Abstract

This paper presents a study of the contact resistance between a metal M (M = Ni, Pt and Au) and an array of n-type Bi₂Te_{3-x}Se_x thermoelectric nanowires deposited by electrodeposition process in alumina membrane. Contact resistances between different metals and thermoelectric nanowires have been tested and characterized after optimization of mechanical thinning and polishing process of the top part of membrane. A low areal contact resistance of 87 $\mu\Omega$ cm² obtained with Au as contact electrode is very encouraging for the development of thermoelectric modules based on nanowires in their membranes.

Keywords

Thermoelectric nanowires, bismuth telluride, contact resistance, thermoelectric device.

I. INTRODUCTION

Bi_2Te_3 and its alloys are well known for their good thermoelectric (TE) performance close to room temperature [1]. Nanostructure engineering progress has further improved their performance, which has drawn much attention on thermoelectric devices [2, 3]. Indeed, low dimensional materials are interesting due to efficiency enhancement by thermal conductivity reduction and their integration into microdevices [4, 5].

Although n and p-type bismuth telluride nanowires (NWs) have been the subject of numerous studies [6-30], only few approaches to build TE devices based on NW have been reported in the literature. Most of these are based on Si or SiGe NWs [31-41] and few on Bi-Te or Bi-Sb-Te NWs [42-45]. Efficiency of TE devices depend on the dimensionless figure of merit $ZT = \alpha^2 T / \rho \lambda$ (with α , ρ , and λ respectively the Seebeck coefficient, electrical resistivity and thermal conductivity) and its electrical contact properties [46].

In the past, different approaches have been used to measure α and ρ and hence the power factor α^2 / ρ . The simplest one involves the use of a two point method which consists to contact both ends of a nanowire. For instance, conducting AFM has been used to measure the power factor of bismuth telluride single nanowires still embedded in their alumina template [47]. Nanoprobng has also been used to characterize the electrical resistivity of n and p-type bismuth telluride nanowires by contacting with a W tip the nucleus generated by the overgrowth of nanowires from the template [48]. Another frequently used approach to measure these parameters is the so-called four point method in which a single nanowire is electrically contacted to four points. Several types of metallic contacts have been studied such as Ni [49], Al [50], Cr/Au [51], or Au/W [52]. The four point method overcomes the problem of the contact resistance unlike the two point method. For the fabrication of thermoelectric devices based on large NW arrays, the problem of the contact resistance becomes crucial.

Contact resistance measurements between large NW assembly in anodic aluminium oxide (AAO) membranes and metal are scarce, even non-existent to our knowledge, and deserve to be studied. Because of the thermoelectrical NWs size close to 60 nm, contact resistances strongly depend of the nanojunctions between thermoelectrical materials and metals. The size of these nanojunctions will strongly depend of the capacities of the metals deposited to reduced the asperities at the interfacial contact. When two rough surfaces are connected together, contact consists of patches of size that can go down to the nanoscale. These junctions at a nanometer scale often exhibit electrical and mechanical properties that diverge

from bulk properties [53]. Various mechanisms such as quantum tunneling [54-56], Sharvin contact [57] and Holm contact [58], depending on the size of contacting junctions and the mean free path of electrons are used to explain transport properties. In addition the nanojunction between rough surfaces can be increased up to a microscale scale under pressure. The size of the patches is strongly dependant of elastic properties of both materials. The inevitable presence of resistive surface films such as oxide layers also contributes to the interfacial resistance. Under sufficient pressure, surface asperities can penetrate the oxide layer thus increasing metal-to-metal contact patches resulting in a relative low resistance.

In this paper, we present a first study of the contact resistance between n-type TE bismuth telluride nanowire and different metals such as Ni, Pt and Au. A mechanical thinning and optimized polishing process of the membrane is firstly presented. The diffusion of deposited metals into TE material is then investigated by EDX analysis before contact resistance measurements of large NW area. The low value of areal contact resistance obtained with gold metal is very interesting for the development of autonomous systems based on micro thermal harvesting.

II. EXPERIMENTAL DETAILS

A. Nanowires growth by electrochemical process and metals deposition

Appropriate $\text{Bi}_2\text{Te}_{3-x}\text{Se}_x$ nanowires leading to n-type semiconducting elements have been developed using pulsed electrodeposition from aqueous solution at room temperature. The electrolyte used is composed of HClO_4 1 M solution containing 10 mM Bi_2O_3 , 10.3 mM TeO_2 and 1.1 mM SeO_2 . Matrix were nanoporous anodic aluminium oxide membranes fabricated by a two-step anodization process in 0.5 M oxalic acid at 40 V, to ensure highly ordered pore arrays [59]. The template thickness and pore diameter are 60 μm and 60 nm respectively. Pulsed electrodeposition conditions, microstructure, composition and TE characterization techniques of electrodeposited nanowires have been detailed in previous works [60,61].

EDX analysis of the n-type nanowire revealed a composition close to $\text{Bi}_{1.45}\text{Te}_{2.85}\text{Se}_{0.7}$. Electron diffraction patterns realized on several isolated nanowires are characteristic of nearly single-crystalline NW in accordance with XRD diffractograms which show a strongly texturation along the [1 1 0] direction. Compositions homogeneity along the length of the NW was verified on single NW using TEM [48] and on NW array after dissolution of the AAO

membrane using EDX technics. A composition variation along the length of the NWs lower than 10% was obtained.

Values obtained for α , ρ and λ are respectively $-78 \mu\text{V} / \text{K}$ [60], $0.29 \text{ m}\Omega \text{ cm}$ [48] and $1.25 \text{ W} / \text{m K}$ [61] at 300 K.

Different metals were deposited on the top part of the AAO membrane using sputtering process. Au metalization necessary for the electrochemical process was kept on the bottom part of the AAO membrane. Three or four spots of 1 mm in diameter and 200 nm in thickness are deposited after surface preparation thinning and etching as described below. Films were deposited at room temperature using a dc magnetron sputtering device. Ni Pt and Au commercial targets of 50 mm diameter were used. Pressure before deposition was lower than $5 \cdot 10^{-6}$ mbar. A 10 min target pre-sputtering was used to eliminate surface contamination prior to plasma deposition. Deposition was realized with DC power fixed to 100, 150 and 200 ± 4 W for respectively Au, Ni and Pt target and with $8 \cdot 10^{-3}$ mbar argon pressure. The reactive ion etching conditions were fixed to 240V /1A with $3 \cdot 10^{-4}$ mbar Ar pressure.

B. Membrane surface preparation

1. Mechanical thinning and optimized polishing process

Differences in nanowires growth rate and unfilled pores lead to membranes partially filled with a non-sharp growth front. It has been shown that pulsing the potential between a deposition potential and a rest one leads to more abrupt growth front [62]. Pulsed regime also leads to more homogeneous chemical composition along the wire axis and improves crystallinity. In our case, pulsed regime has ensured a better filling ratio. Surface mechanical thinning and polishing are still necessary to overcome the $20 \mu\text{m}$ of unfilled pores, as shown in fig.1.a.

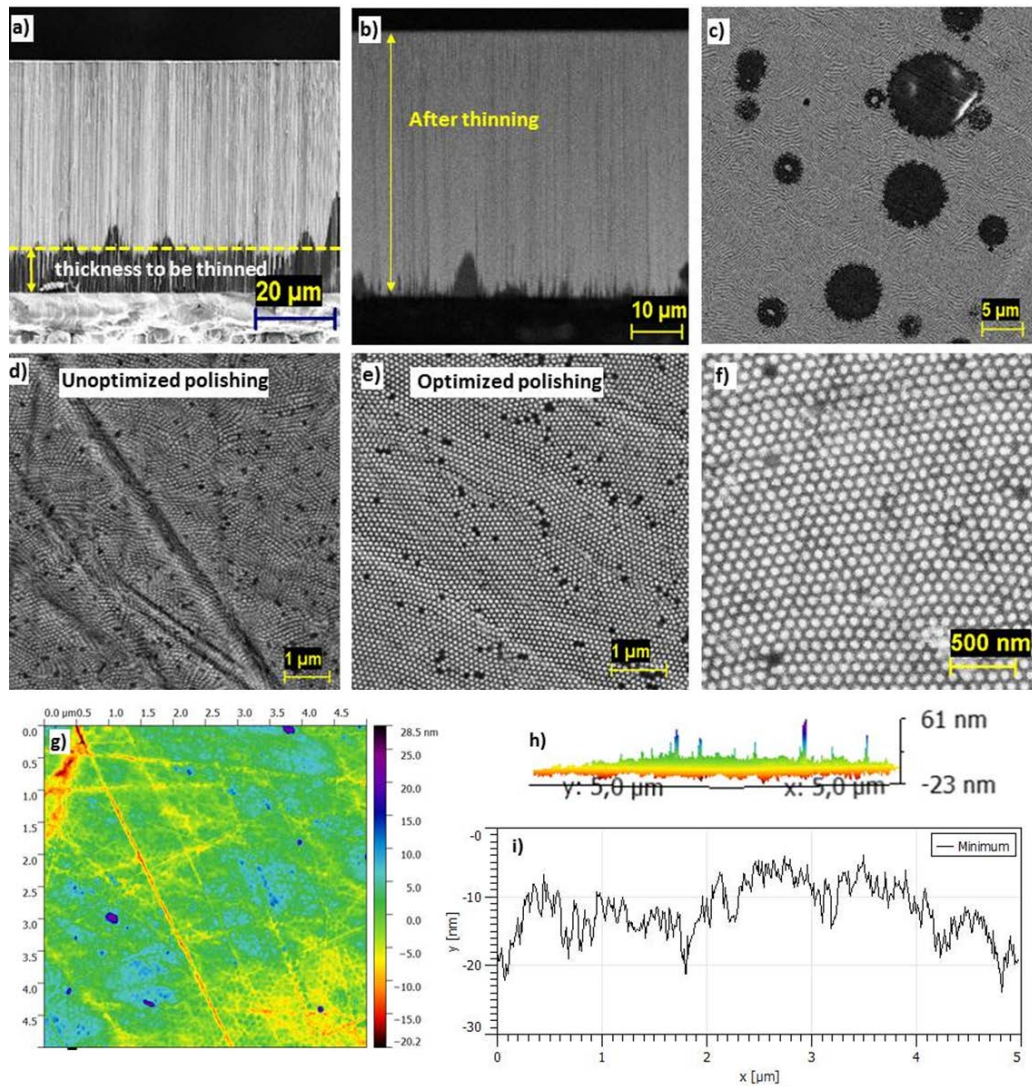


Figure 1 : (a,b) SEM images of the membranes in cross-section before and after thinning and polishing (c-f) SEM images of surfaces after thinning and polishing. (g) AFM topography on a polished surface ($5 \times 5 \mu\text{m}^2$). (h) 3D topography (i) Depth profile of polishing marks (in nm).

Membrane brittleness makes polishing process a critical step due to porosity, thickness and stresses during electrochemical deposition. Many membranes break during polishing if the process is not optimized. In this context, we developed a special sample holder and a constant pressing process leading to a planar and homogenous polishing and to avoid membranes loss (Fig.1b/c). Different grain size abrasives and polishing durations were also studied to optimize the surface quality finish (Fig. 1e/f) and to avoid deep and irregular polishing marks (Fig. 1d). Only mechanical polishing is applied on the face with overgrown material (the back side corresponding to the bottom of the membrane being still covered by gold used as contact electrode for electrochemical deposition of the material). It starts with a grit paper of 1200,

down to 4000 and finishing is done with diamond paste of 1 μ m. No chemical nor electrochemical polishing was used at this step. As evidenced by SEM pictures of Fig 1e/f, no SiC grain incorporated in the alumina filled surface after polishing can be observed.

AFM topographic analysis were performed to estimate the depth of the polishing marks as shown in Fig. 1g/h. Analysis on different spots of 25 μ m² high quality surface show a good planarity distribution with marks depth lower than 10 nm (Fig 1i).

2. *Impact of surface RIE (reactive ion etching)*

The second crucial step of samples surface preparation is ion etching before contact metal deposition. It removes the oxide layer on the polished surface and improves the metallic contact at the nanowire tips.

Areal contact resistance ρ_c calculated with equations 1-4 was studied for different etching durations to optimize oxide layer removal. A constant thickness metal of 200 nm was chosen for this study. Samples with no etching revealed high ρ_c (6.7 m Ω .cm²) which confirms etching as a key parameter.

Best results are obtained for 30 s and 90 s leading to ρ_c lower than 500 $\mu\Omega$.cm². Very high etching durations (2 à 7 min) induced higher ρ_c (up to 1 m Ω .cm²) These high ρ_c values are explained by sample surface heating during etching, leading to a local composition modification of Bi₂Te_{3-x}Se_x. Additional depositions with different contact metals were then processed on both type of etched samples (30 s and 90 s etching duration). The best areal contact resistance of 200 $\mu\Omega$.cm² was obtained for 90 s etching time. This duration was adopted for the rest of the study.

III. RESULTS

A. Study of metal diffusion

In order to complete our study, we focused on samples surface analysis after metal deposition. Figure 2 shows captions of AFM surface analysis (25 μ m²) after each metal deposition (Au, Ni and Pt). Topography results show that maximum depth of polishing marks is around 20 nm. The contact deposition process used for NWs is of high quality, no metal delamination is observed as for thermoelectric films [63].

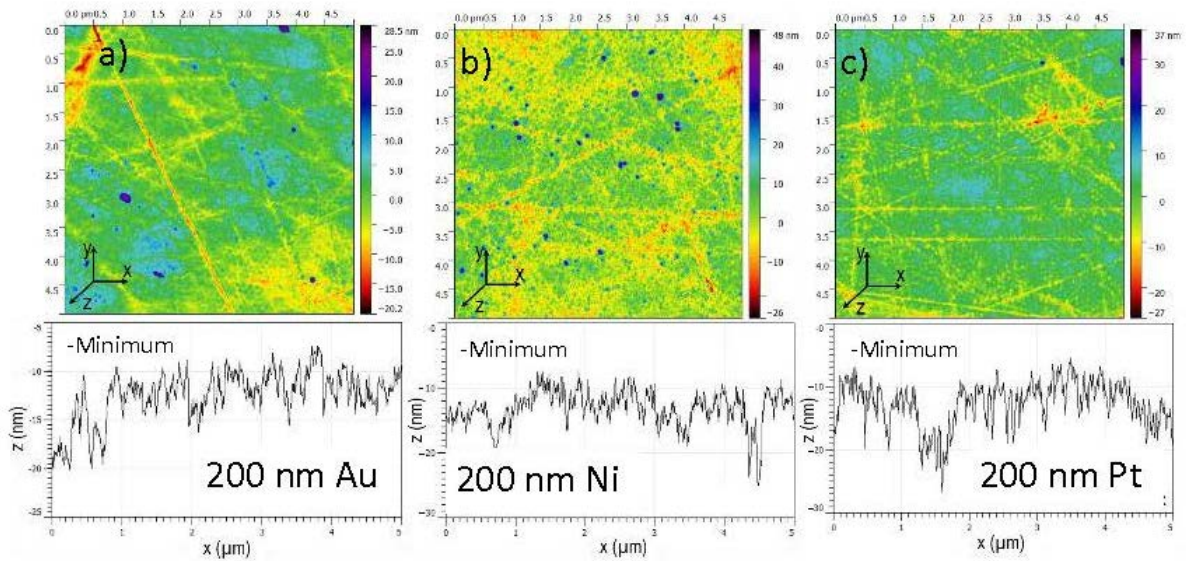


Figure 2: AFM topography of the different surfaces after deposition of Au (a), Ni (b) and Pt (c).

Diffusion of deposited metals into TE material was also investigated. Characterization process issues complicated the study of metal diffusions at the nanometric scale. It was still possible to establish a micrometric investigation of Ni diffusion described by the concentration evolution profile (fig. 3a and 3b).

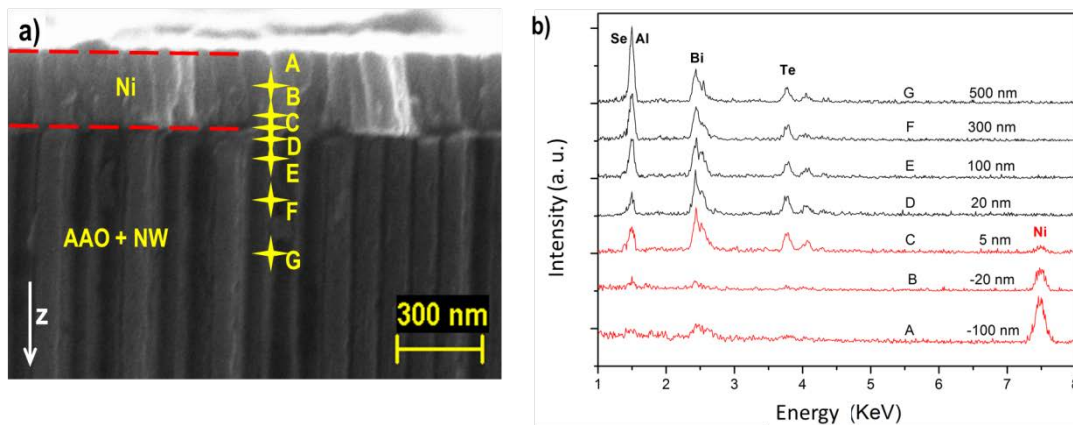


Figure 3: (a) Cross section image of the Ni/NWs interface. EDX analysis points are visible in yellow (b) EDX spectra at the analysis points.

Further study was conducted on Ni diffusion into samples. Polished TE material with 200nm thick Ni deposits were analyzed by MEB-EDX on cross-section at the interface. Fig.3.a shows the microstructure of the contact region (cross-section) between the Ni metallization

layer and TE nanowires. A sharp separation and no additional layer is observed between the Ni and NW illustrating a low Ni diffusion into the sample and no formation of intermediate component. These conclusions are confirmed by EDX spectra obtained on different analysis points on both sides of the contact region as shown on fig.3b. For points D to G, the electronic analysis beam was centered on an emerging Bi-Te-Se NW after fracture. According to Monte Carlo simulation, the interaction volume of the analysis electron beam is estimated to 100 nm and can be represented by uncertainty bars on the position x. In this condition the small Ni concentration found at the +5nm could be due to the analysis rather than to a real diffusion of Ni in the Bi-Te-Se NW. Despite these difficulties of analysis, it seems that the Ni peak appears at 5 nm from the contact region and disappears 20 nm further.

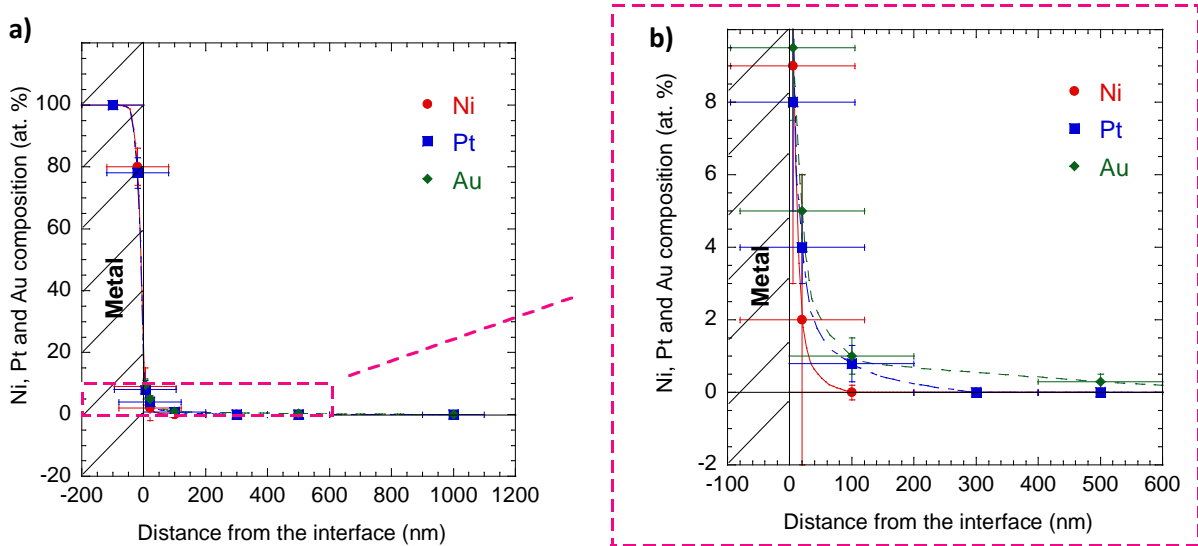


Figure 4 : (a) Variation of Ni, Pt, Au concentrations as a function of the distance from the interface. (b) Zoom of a part of the fig. 4a delimited by red dashes.

Figure 4 shows that the diffusion is increased for Pt and Au. The concentrations in Pt and Au become close to zero at a distance of respectively 0.5 and 1 μm from the interface (figure 4b).

B. Areal contact resistances ρ_c measurements

The electrical contact resistance was measured with a scanning voltage probe set up at room temperature and at atmospheric pressure under air. The voltage drop along a TE NW is measured as a small current passes through the element. The diameter of the circular spot for resistance measurement is 1 mm and a current varying from 0 to 10 mA is applied. The measurement is made with the current flowing in the forward direction (from the top to the

bottom of the NWs) then a second measurement is made with the current in the reverse direction in view to subtract any thermal electromotive force. The temperature rise induced by Joule effect is estimated to be less than 0.5K. Figure 5 shows the experimental set up for the contact resistance measurements.

The force exerted by the point of our measurement resistance set up was determined using a commercial accuracy balance. The maximum of the force measured is 0.3 N. The maximum stress applied to the contact is 1.5 MPa according to a point surface of 0.2 mm².

During the measurement of our samples, by increasing the force of the point on the contact, the resistance passes sharply from insulating to conducting. Once contact has been established, no resistance variation versus the pressure is observed. We concluded that the pressure as no influence on the resistance measurements.

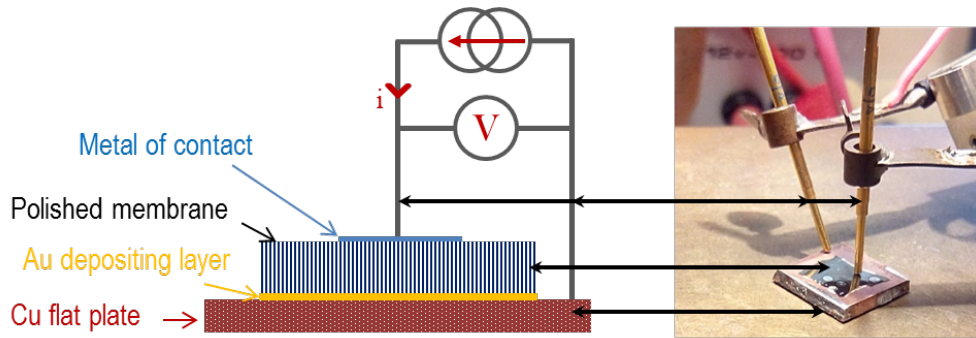


Figure 5: Experimental set up for contact resistance measurements.

The contact resistance can be calculated according to equation 1.

$$R_{measured} = \frac{V}{i} = R_{NW} + R_{set_up} + R_c^{sup} + R_c^{inf} \quad (Eq. 1)$$

with R_{NW} the NW electrical resistance and R_{set_up} the set-up resistance. R_c^{sup} and R_c^{inf} correspond respectively to the electrical contact resistance of the metal/NW heads and metal/NW feet. Voltage probes were optimized in order to cancel the contribution of R_{set_up} estimated to 1 m Ω (2 retractable tips of 1.5 mm long and 0.8 mm in diameter). According to the electrochemical process for Au metalization of the bottom part of the AAO membrane, it was assumed that $R_c^{inf} \ll R_c^{sup}$. Contact resistance R_c and areal contact resistance ρ_c are calculated with equations (2) and (3)

$$R_c = R_c^{sup} = R_{measured} - R_{NW} \quad (Eq. 2)$$

$$\rho_c = R_c \cdot S_{NW} \quad (Eq. 3)$$

with S_{NW} the contact area of connected NWs which can be obtained with equation (4)

$$S_{NW} = d \cdot S_{plot} \quad (Eq. 4)$$

where d is the areal NWs density .

With the AAO prepared for this study and $S_{plot} = 0.785 \text{ mm}^2$, S_{NW} is close to $2.35 \times 10^{-3} \text{ cm}^2$.

In previous studies [48], electrical resistivity is determined as $0.29 \text{ m}\Omega\cdot\text{cm}$. NWs density and dimension lead to R_{NW} of $0.56 \times 10^{-3} \Omega$.

Table 1 summarizes the areal contact resistances of the studied metals (Pt, Ni and Au) deposited by sputtering (200 nm) with 90 s etching time. Results show the lowest areal contact resistance for Au with a value of $87 \mu\Omega\cdot\text{cm}^2$. Pt and Ni also show low values, in the range of several hundreds of $\mu\Omega\cdot\text{cm}^2$.

Metal	Ni	Pt	Au
$R_{\text{measured}} (\Omega)$	0.1	0.08	0.038
$R_{NW} (\Omega)$	0.56×10^{-3}	0.56×10^{-3}	0.56×10^{-3}
$R_c (\Omega)$	0.099	0.079	0.037
$\rho_c (\mu\Omega\cdot\text{cm}^2)$	232	185	87

Table 1: Areal contact resistances ρ_c obtained for the different metals studied. R_{NW} has been determined using electrical resistivity measured in ref [48] and NW dimensions.

We also studied the impact of an adhesion layer on the electrical resistance. A deposition of 10 nm of W shows an increase of contact resistance in comparison with samples metalized directly. Adding to its high diffusion behaviour, we considered that the W layer was not necessary or even harmful to obtaining low contact resistance.

The low value obtained for Au metal contacts is crucial for performance improvement of TE modules. It is comparable to those obtained in the literature on Bi_2Te_3 TE elements based on bulk [64,65] and thin films [66] with Ni or Bi-Sn as contact metal between Bi_2Te_3 and electrodes.

The lowest contact resistances were reported by Gupta et al. They obtained values of about $5 \mu\Omega\cdot\text{cm}^2$ on $\text{Bi}_2\text{Te}_3/\text{Ni}$ and $\text{Sb}_2\text{Te}_3/\text{Ni}$ interfaces [67]. This value was subsequently improved

to a value lower than $0.1 \mu\Omega\text{-cm}^2$ on thin layers of Bi_2Te_3 with Ni and Co as contact metals [68]. The high contact resistance of the NW/Ni interfaces could be due to a less pronounced diffusion in the BiTeSe NW compound than for Au and Pt. The effects of recombination between oxygen from AAO membrane and Ni elements leading to nickel oxide formation are also not to be neglected to explain these high value compared to those of the literature.

IV. CONCLUSION

Different metals such as Ni, Pt and Au have been studied for the optimization of the contact resistance between $\text{Bi}_2\text{Te}_{3-x}\text{Se}_x$ NW in AAO membrane and electrodes. EDX analysis shows that the highest diffusion is for Au, whereas the diffusion depth of Ni is lower than 15 nm. After focusing on surface preparation of the NW still embedded in the AAO membrane and etching conditions, a low areal contact resistance of $87 \mu\Omega \text{ cm}^2$ has been obtained with Au metal contact. Such results are very encouraging for the development of thermoelectric modules based on nanowires in their membranes.

Data Availability

The data that support the findings of this study are available from the corresponding author upon reasonable request.

Acknowledgements

This work was financially supported by the CIFRE process (N° 2013/0149) provided by the ANRT which is gratefully acknowledged. The authors thank ST Microelectronics for their collaboration in this work. The authors would like to thank the technical support and discussions provided by the “Pôle Capteur” and “Pôle Optique et Microscopie” facilities in Institut Néel at CNRS-Grenoble.

References

- [1] H. J. Goldsmid, R. W. Douglas, *Brit. J. of Appl. Phys.* **5** 386 (1954).
- [2] R. Venkatasubramanian, T. Colpitts, E. Watko, M. Lamvik, N. El-Masry, *J. Cryst. Growth* **170** 817 (1997).
- [3] R. Venkatasubramanian, E. Siivola, T. Colpitts, B. O'Quinn, *Nature* **413** 597 (2001).
- [4] L.D. Hicks, T.C. Harman, M.S. Dresselhaus, *Appl. Phys. Lett.* **63**, 3230 (1993).
- [5] L.D. Hicks, M.S. Dresselhaus, *Phys. Rev. B* **47** 16631 (1993).
- [6] J. Fleurial A. Borshchevsky, M.A.Ryan, W.M. Philips, J.G. Snyder, T. Caillat, E.A. Kolawa, J.A. Herman, P. Mueller, M. Nicolet, *Mater. Res. Soc.*, **545**, 493 (1999).
- [7] S. A. Sapp, B. B. Lakshmi et C. R. Martin, *Adv. Mater.* **11**, 402 (1999).
- [8] W. Wang, Q. Huang, F. Jia, J. Zhu, *J. Appl. Phys.* **96** 615 (2004).
- [9] R. Mannam, M. Agarwal, A. Roy, V. Singh, K. Varahramyan, D. Davis, *J. Electrochem. Soc.* **156** B871 (2009).
- [10] C. Frantz, N. Stein, L. Gravier, S. Granville, C. Boulanger, *J. Electr. Mat.* **39** 2043 (2010).
- [11] K. Tittes, W. Plieth, *J. Solid State Electrochem.* **11** 155 (2007).
- [12] M. Martin-Gonzalez, A. Prieto, R. Gronsky, T. Sands, A. Stacy, *Adv. Mater.* **15** 1003 (2003).
- [13] F. Xiao, B. Yoo, K.-H. Lee, N. V. Myung, *Nanotechnology*, **18** (33) 335203 (2007).
- [14] X. Li, E. Koukharenko, I. Nandhakumar, J. Tudor, S. Beeby, N. White, *Phys. Chem. Chem. Phys.* **11** 3584 (2009).
- [15] M. Martin-Gonzalez, G. J. Snyder, A. L. Prieto, R. Gronsky, T. Sands, A. M. Stacy, *Nano Lett.* **3** 973 (2003).
- [16] S. Bäßler, T. Böhnert, J. Gooth, C. Schumacher, E. Pippel, K. Nielsch, *Nanotechnology* **24** 495402 (2013).
- [17] M. Tan, Y. Deng, Y. Wang, *Nano Energy* **3** 144 (2014).
- [18] G. Zhang, B. Kirk, L. A. Jauregui, H. Yang, X. Xu, Y. P. Chen, Y. Wu, *Nano Lett.* **12** 56 (2012).
- [19] C. V. Manzano, J. Martin, M. S. Martin-González, *Microporous Mesoporous Mat.* **184** 177 (2014).
- [20] M. S. Sander, A. L. Prieto, R. Gronsky, T. Sands, A. M. Stacy, *Adv. Mater.* **14** 665 (2002).
- [21] L. Trahey, C. R. Becker, A. M. Stacy, *Nano Lett.* **7** 2535 (2007).

- [22] L. Li, Y. Yang, X. Huang, G. Li, L. Zhang, *Nanotechnology* **17** 1706 (2006).
- [23] J. Lee, S. Farhangfar, J. Lee, L. Cagnon, R. Scholz, U. Gosele, K. Nielsch, *Nanotechnology* **19** 365701 (2008).
- [24] W.-L. Wang, C.-C. Wan, Y.-Y. Wang, *J. Phys. Chem. B* **110** 12974 (2006).
- [25] N. Peranio, E. Leister, W. Töllner, O. Eibl, K. Nielsch, *Adv. Func. Mater.* **22** 151 (2012).
- [26] J. Klammer, J. Bachmann, W. Tollner, D. Bourgault, L. Cagnon, U. Gosele, K. Nielsch, *Phys. Status Solidi B* **247** 1384 (2010).
- [27] W. Wang, G. Zhang, X. Li, *J. Phys. Chem. C* **112** 15190 (2008).
- [29] C. Hsin, M. Wingert, C. Huang, H. Guo, T. Shih, J. Suh, K. Wang, J. Wu, W. Wu, R. Chen, *Nanoscale* **5** 4669 (2013).
- [30] E. J. Menke, M. A. Brown, Q. Li, J. C. Hemminger, R. M. Penner, *Langmuir* **22** 10564 (2006).
- [31] A. Ali, Y. Chen, V. Vasiraju, S. Vaddiraju, *Nanotechnology* **28** 282001 (2017).
- [32] B.M. Curtin, E.W. Fang, J.E. Bowers, *J. Electron. Mater.* **41** 887 (2012).
- [33] M. Tomita, S. Oba, Y. Himeda, R. Yamato, K. Shima, T. Kumada, M. Xu, H. Takezawa, K. Mesaki, K. Tsuda, S. Hashimoto, T. Zhan, H. Zhang, Y. Kamakura, Y. Suzuki, H. Inokawa, H. Ikeda, T. Matsukawa, T. Matsuki, T. Watanabe, *IEEE Trans. Electron Devices* 1–9 (2018).
- [34] D. Dávila, A. Tarancón, C. Calaza, M. Salleras, M. Fernández-Regúlez, A. San Paulo, L.L. Fonseca, *Nano Energy* **1** 812 (2012).
- [35] B. Xu, K. Fobelets, 2014 *J. Appl. Phys.* **115** 214306. [36] K.J. Norris, M.P. Garrett, J. Zhang, E. Coleman, G.S. Tompa, N.P. Kobayashi, *Energy Convers. Manag.* **96** 100 (2015).
- [37] L. Fonseca, J.D. Santos, A. Roncaglia, D. Narducci, C. Calaza, M. Salleras, I. Donmez, A. Tarancon, A. Morata, G. Gadea, L. Belsito, L. Zulian, *Semicond. Sci. Technol.* **31** 084001 (2016).
- [38] G. Pennelli, M. Totaro, M. Piotto, P. Bruschi, *Nano Lett.* **13** 2592 (2013).
- [39] Zhan T, Yamato R, Hashimoto S, Tomita M, Oba S, Himeda Y, Mesaki K, Takezawa H, Yokogawa R, Xu Y, Matsukawa T, Ogura A, Kamakura Y, Watanabe T. *Sci. Technol. Adv. Mater.* **24** 443 (2018).
- [40] Inci Donmez Noyana, Gerard Gadeab, Marc Sallerasa, Merce Paciosb, Carlos Calazaa, Andrej Stranza, Marc Dolceta, Alex Moratab, Albert Taranconb,c, Luis Fonseca, *Nano Energy* **57** 492 (2019).
- [41] J. Choi, K. Cho, S. Kim, *Adv. Energy Mater.* **7** 1602138 (2017).

- [42] J. R. Lim, J. F. Whitacre, J.-P. Fleurial, C.-K. Huang, M. A. Ryan, N. V. Myung, *Adv. Mater.* **17** 1488 (2005).
- [43] F. Domínguez-Adamea, M. Martín-González, D. Sánchez, A. Cantarero, *Physica E Low Dimens. Syst. Nanostruct.* **113** 213 (2019).
- [44] E. Koukharenko, S. A. Boden, N. P. Sessions, N. Frety, I. Nandhakumar, N. M. White, *J. Mater. Sci. Mater. Electron.* **29** 3423 (2018).
- [45] M. Y. Kim, K. W. Park, T. S. Oh, *J. Korean Inst. Metals Mater.* **47** 248 (2009).
- [46] P. Jones, T. E. Huber, J. Melngailis, J. Barry, M. H. Ervin, T.S. Zheleva, A. Nikolaeva, Leonid Konopko, M. Graf, 25th International Conference on Thermoelectrics (2006).
- [47] J. Lee, Y. Kim, L. Cagnon, U. Gösele, J. Lee, K. Nielsch, *Phys. Status Solidi RRL* **4**, 43 (2010).
- [48] M. Ben Khedim, L. Cagnon, C. Garagnon, V. Serradeil, D. Bourgault, *Phys. Chem. Chem. Phys.* **18** 12332 (2016).
- [49] D. Kojda, R. Mitdank, A. Mogilatenko, W. Töllner, Z. Wang, M. Kröner, P. Woias, K. Nielsch, S. F. Fischer, *Semicond. Sci. Technol.* **29** 124006 (2014).
- [50] H. S. Shin, S. G. Jeon, J. Yu, Y. S. Kim, H. M. Park, J. Y. Song, *Nanoscale* **6** 6158 (2014).
- [51] T. Chang, S. Cho, J. Kim, J. Schoenleber, C. Frantz, N. Stein, C. Boulanger, W Lee. *Electrochim. Acta* **161** 403 (2015).
- [52] M. Muñoz Rojo, Y. Zhang, C. V. Manzano, R. Alvaro, J. Gooth, M. Salmeron, M. Martín-González, *Sci. Rep.* **6** 19014 (2016).
- [53] R. L., Jackson, E. R., Crandall, M. Bozack, *Proc., Electrical Contacts (Holm), 2012 IEEE 58th Holm Conf. on, IEEE, New York, 1–10* (2012).
- [54] A. Yanson, G. R., Bollinger, H. Van den Brom, N. Agrait, J. Van Ruitenbeek *Nature* **395** (6704), 783 (1998).
- [55] E. Foley, D. Candela, K. Martini, M. Tuominen, *Am. J. Phys.* **67**(5) 389 (1999).
- [56] Y. V. Sharvin, *Zh. Eksperim. i Teor. Fiz.* **48** 984 (1965).
- [57] N. Agrait, A. L. Yeyati, J. M. Van Ruitenbeek, *Phys. Rep.* **377**(2) 81 (2003).
- [58] R. Holm, E. A. Holm, *Electric contacts*, Springer, New York (1967).
- [59] H. Masuda, K. Fukuda, *Science* **268** 1466 (1995).
- [60] M. Ben Khedim, L. Cagnon, V. Serradeil, T. Fournier, D. Bourgault, *Materials Today: Proceedings* **2** 60 (2015).

- [61] D. Singhal, J. Paterson, M. Meriam Ben-Khedim, D. Tainoff, L. Cagnon, J. Richard, E. Chavez-Angel, J. Jaramillo-Fernandez, C. M. Sotomayor-Torres, D. Lacroix, D. Bourgault, D. Buttard, O. Bourgeois, *Nanoscale* **11** 13423(2019).
- [62] K. Nielsch, F. Müller, A. P. Li, U. Gösele, *Adv. Mater.* **12** 582 (2000).
- [63] D. Bourgault, C. Giroud Garampon, N. Caillault, L. Carbone, *Sens. Actuators A Phys.* **273** 84 (2018).
- [64] O. J. Mengali, M. R. Seiler, *Adv. Energy Convers.* **2** 59 (1962).
- [65] R. J. Buist, S. J. Roman, 18th International Conference on Thermoelectrics, International Thermoelectric Society, Baltimore, MD (1999).
- [66] S. J. Kim, J. H. Wea, B. J. Cho, *Energy Environ. Sci.* **7** 1959 (2014).
- [67] R. Gupta, J. White, O. Iyore, U. Chakrabarti, H. N. Alshareef, B. Gnade, *Electrochem. Solid-State Lett.* **12** H302 (2009).
- [68] R. P. Gupta, K. Xiong, J. B. White, K. Cho, H. N. Alshareef, B. E. Gnade, *Journal of The Electrochemical Society*, **157** H666 (2010).